

De Novo Synthesis of Dihydrobenzofurans and Indolines and Its Application to a Modular, Asymmetric Synthesis of Beraprost

Ze-Shu Wang,[§] Steven H. Bennett,[§] Bilal Kicin,[§] Changcheng Jing, Johan A. Pradeilles, Karen Thai, James R. Smith, P. David Bacoş, Valerio Fasano, Carla M. Saunders, and Varinder K. Aggarwal*



Cite This: <https://doi.org/10.1021/jacs.3c04582>



Read Online

ACCESS |



Metrics & More

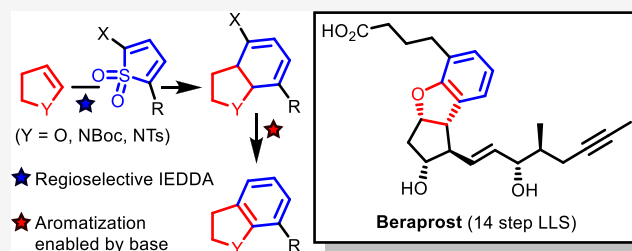


Article Recommendations



Supporting Information

ABSTRACT: Dihydrobenzofurans and indolines are important constituents of pharmaceuticals. Herein, we describe a novel strategy for their construction in which the aromatic ring is created *de novo* through an inverse-electron demand Diels–Alder reaction and cheletropic extrusion sequence of a 2-halothiophene-1,1-dioxide with an enol ether/enamide, followed by aromatization. Unusually, the aromatization process proved to be highly challenging, but it was discovered that treatment of the halocyclohexadienes with a base effected an α -elimination–aromatization reaction. Mechanistic investigation of this step using deuterium-labeling studies indicated the intermediacy of a carbene which undergoes a 1,2-hydrogen shift and subsequent aromatization. The methodology was applied to a modular and stereoselective total synthesis of the antiplatelet drug beraprost in only 8 steps from a key enal-lactone. This lactone provided the core of beraprost to which both its sidechains could be appended through a 1,4-conjugate addition process (lower ω -sidechain), followed by *de novo* construction of beraprost's dihydrobenzofuran (upper α -sidechain) using our newly developed methodology. Additionally, we have demonstrated the breadth of our newly established protocol in the synthesis of functionalized indolines, which occurred with high levels of regiocontrol. According to density-functional theory (DFT) calculations, the high selectivity originates from attractive London dispersion interactions in the TS of the Diels–Alder reaction.



INTRODUCTION

Pulmonary arterial hypertension (PAH) is a rare and incurable cardiovascular disease (CVD) that is characterized by high blood pressure in the arteries of the lungs, which ultimately leads to right ventricular heart failure and premature death.¹ Typical treatment for this life-threatening illness involves the administration of the potent anti-hypertensive, prostacyclin (PGI₂, epoprostenol, **2**).² Unfortunately, due to the short metabolic half-life of PGI₂ in blood ($t_{1/2}$ = 3–6 min)³ continuous intravenous (IV) infusion is required.² To address the practical issues associated with such treatment, a number of more stable PGI₂ analogues have been developed, e.g., cicaprost,⁴ iloprost⁵ and more recently, beraprost (**1**)⁶ (Figure 1).

Beraprost (beraprost sodium, **1**)⁷ is a more stable ($t_{1/2}$ = 60 min) and less cytotoxic prostacyclin analogue and can be administered orally. It has been used successfully in the treatment of peripheral arterial disease (Buerger's disease and arteriosclerosis obliterans) and shows promise as a potential therapeutic for the treatment of PAH due to its ability to drastically reduce pulmonary arterial pressure and resistance.⁷

Most strategies for the enantioselective synthesis of beraprost have focused on using either resolution strategies,⁸ or the enantiopure (–)-Corey lactone.⁹ Recently, Hayashi,¹⁰

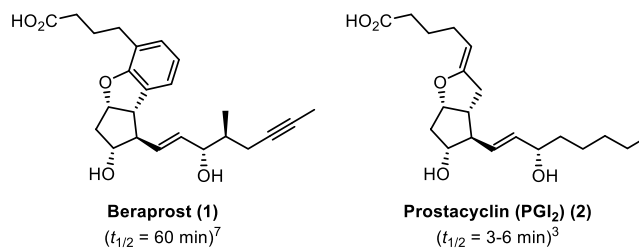


Figure 1. Structural comparison of beraprost (**1**) vs prostacyclin (PGI₂, **2**).

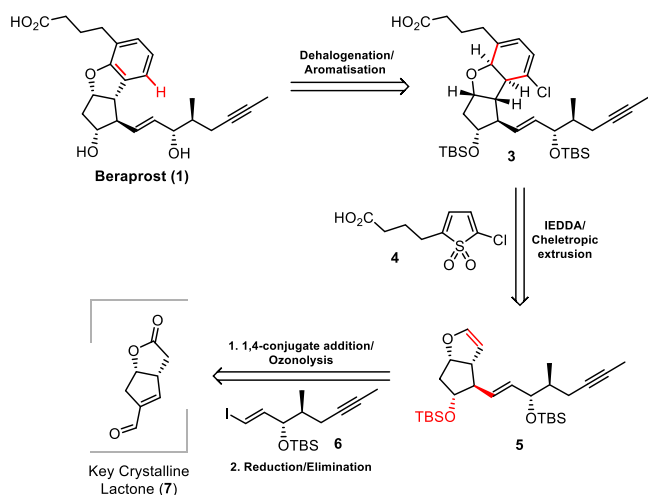
reported an asymmetric organocatalytic synthesis of beraprost through a formal [3+2] cycloaddition reaction catalyzed by diphenylprolinol silyl ether as the key step to construct the cyclopentane core.¹¹ We have previously reported enantioselective syntheses of several prostanoids from enal-lactone **7** (or

Received: May 3, 2023

the related hemi-acetal), which is prepared by a stereo-controlled organocatalytic dimerization of succinaldehyde in 3 steps with >99% e.e.¹² We were keen to broaden the reach of this chemistry further and now report its use in a 14 step [longest linear sequence (LLS)] synthesis of beraprost. Furthermore, during the course of the synthesis, we discovered a conceptually novel route to access dihydrobenzofurans, which we demonstrate is more general and can also be applied to the *de novo* synthesis of indolines.

Retrosynthetic Analysis. In terms of retrosynthesis, we envisaged a modular approach involving three key building blocks: enal-lactone **7**, upper α -sidechain **4**, and lower ω -sidechain **6**. The upper α -sidechain was proposed to be installed through an inverse-electron demand Diels–Alder reaction (IEDDA) between enol ether **5** and thiophene-1,1-dioxide **4**, followed by cheletropic extrusion of SO₂. Subsequent dehalogenation and aromatization would furnish beraprost's dihydrobenzofuran core. The lower ω -sidechain could be introduced through a 1,4-conjugate addition of vinyl iodide **6** and key enal-lactone **7** (Scheme 1). A critical issue

Scheme 1. Proposed Modular Retrosynthetic Analysis of Beraprost



that we were uncertain about initially was the regiochemistry of the IEDDA process, as most Diels–Alder reactions of thiophene 1,1-dioxides use symmetrical substrates.^{13a–d} Additionally, monosubstituted thiophene 1,1-dioxides are known to be unstable and prone to rapid cyclodimerization.^{13e,f} We therefore decided to introduce a halogen substituent in the 2-position to stabilize the thiophene 1,1-dioxide, which, in addition, would also lower the LUMO of the diene for the IEDDA.¹⁴ Such a substituent would also be easily removable at a later stage.

RESULTS AND DISCUSSION

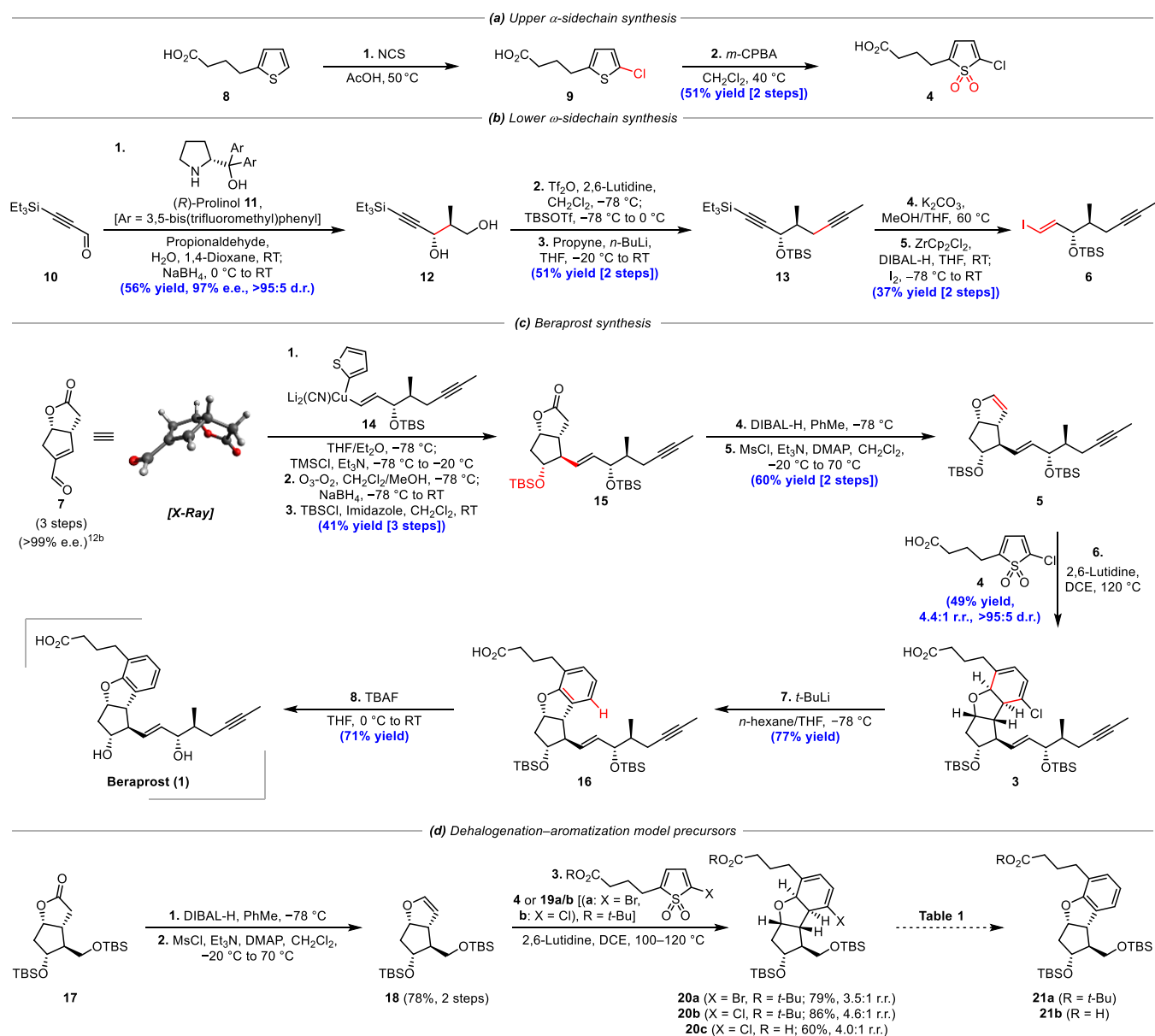
Asymmetric Synthesis of Beraprost. Starting from commercially available thiophene **8**, we prepared thiophene 1,1-dioxide **4** in two steps following a regioselective chlorination using *N*-chlorosuccinimide (NCS) and subsequent oxidation with *meta*-chloroperoxybenzoic acid (*m*-CPBA) (Scheme 2a). This afforded the desired upper α -sidechain in 51% yield on a gram scale. The lower ω -sidechain (Scheme 2b) required for 1,4-conjugate addition was prepared from ynal **10**,¹⁵ which itself could be synthesized on a

decagram scale from (triethylsilyl)acetylene. Ynal **10** readily underwent a prolinol-catalyzed aldol reaction with propionaldehyde,¹⁶ followed by *in situ* reduction with NaBH₄ to give diol **12** with near-perfect enantioselectivity (98.5:1.5 e.r.) and high diastereoselectivity (9.1:1 d.r.) that was improved to >95:5 d.r. following flash column chromatography. The primary alcohol of diol **12** was then selectively transformed into a triflate and the remaining secondary alcohol was protected as its corresponding *tert*-butylsilyl (TBS) ether. This allowed for the selective substitution of the triflate with propynyllithium to afford di-alkyne **13** in 51% over two steps. Subsequent alkyne deprotection under basic conditions followed by hydrozirconation/iodination of the resultant terminal alkyne produced vinyl iodide **6** in 37% over two steps.

Following gram-scale synthesis of enal-lactone **7**,^{12b} and with vinyl iodide **6** in hand, the 1,4-conjugate addition of *in situ*-generated higher-order cyanocuprate **14** was performed (Scheme 2c). Following 1,4-addition onto the enal of **7** and trapping with trimethylsilyl chloride (TMSCl), a TMS enol ether was produced, which was perfectly set up to undergo selective ozonolysis of the more electron-rich alkene. Subsequent reductive work-up with NaBH₄ and TBSCl protection delivered protected secondary alcohol **15** in 41% yield over 3 steps as a single diastereomer. The high stereocontrol observed in this sequence is a consequence of the convex shape of enal-lactone **7**, which favors attack from the more exposed *exo* face (see the X-ray structure). The lactone moiety of **15** was reduced with DIBAL-H to give a hemiacetal, which, following mesylation and subsequent heating under reflux, underwent elimination to produce enol ether **5** in 60% yield over 2 steps. Heating enol ether **5** in the presence of thiophene 1,1-dioxide **4** and 2,6-lutidine effected the desired IEDDA/cheletropic extrusion process giving chlorocyclohexadiene **3** in 49% yield and 4.4:1 regioisomeric ratio (r.r.). We believe the selectivity is controlled by steric repulsion between the two long linear sidechains rather than by any possible electronic effects (*vide infra*). Indeed, the more hindered *t*-Bu ester of thiophene 1,1-dioxide **4** gave the corresponding chlorocyclohexadiene with an improved 5.2:1 r.r. The success of the IEDDA reaction provided vindication of our strategy since we were only a few steps from beraprost. However, the seemingly facile oxidation of the diene to the aromatic ring, which can often occur spontaneously in air,¹⁷ was unexpectedly found to be the most challenging step in the synthesis.

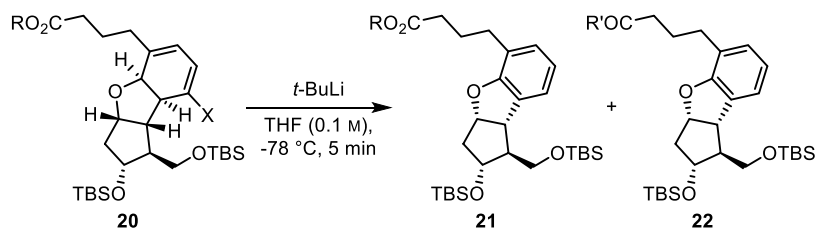
Dehalogenation–Aromatization of the Model System. To further explore and optimize our dehalogenation–aromatization step, we used the simple model compounds **20a–c**, prepared from cycloaddition of (–)-Corey lactone derived enol ether **18** with various thiophene-1,1-dioxides in moderate regioselectivity (**20a**, 3.5:1 r.r.; **20b**, 4.6:1 r.r.; **20c**, 4.0:1 r.r.) (Scheme 2d). We initially tested the bromo-diene and *tert*-butyl protected ester form (**20a**), which we believed would be easier to guide our initial efforts toward aromatization. At first, we focused on the use of palladium or platinum catalysis to effect simultaneous aromatization and dehalogenation (a redox neutral process), but unfortunately, we observed decomposition under the majority of conditions.^{9,18} No aromatization was observed under a number of other conditions: DBU/air,¹⁹ DDQ,²⁰ KMnO₄·Al₂O₃,²¹ MnO₂,²² and PdCl₂/HSi(OEt)₃.²³ In fact, in many cases, aromatization by elimination of the alcohol occurred rather than oxidation.²⁴ Indeed, a survey of the literature revealed

Scheme 2. Modular Asymmetric Synthesis of Beraprost



that similar *cis*-fused 5,6-cyclohexadiene ring systems often show remarkable resistance toward aromatization, requiring either novel strategies^{25a} or harsh conditions^{25b,c} to effect the transformation. Furthermore, our system incorporated an additional steric challenge with the ring-junction hydrogens presenting into the concave face of the molecule, making their removal more difficult. At this point, we wanted to determine if the halogen (bromide) was somehow inhibiting aromatization and as such sought the bromide-free cyclohexadiene. Thus, bromocyclohexadiene **20a** was subjected to a lithium–halogen exchange reaction using 2.0 equiv of *tert*-butyllithium (*t*-BuLi) in THF at $-78\text{ }^{\circ}\text{C}$, followed by quenching with MeOH. However, surprisingly, the expected lithium–halogen exchange product was not observed. Instead, the highly sought-after aromatic product **21a** was found in 7% yield alongside the *tert*-butyl ketone derivative **22**, formed by over-reaction of the excess *t*-BuLi (Table 1, entry 1).

Optimization of Dehalogenation–Aromatization and Completion of the Synthesis. This discovery provided a potential solution to our problem and so we set about optimizing the process. Through optimization, we found that our desired aromatic product could be obtained in increasing yield by (i) switching from THF to a cosolvent system of *n*-hexane:THF (95:5) (entry 2), (ii) increasing the equivalents of *t*-BuLi (entry 3), and (iii) replacing the bromide with a chloride (entry 4). This afforded a 56% yield of the desired product but together with an increased 32% yield of the undesired *tert*-butyl ketone product. Using the carboxylic acid instead of the ester, the undesired *tert*-butyl ketone product could be avoided, giving the desired aromatic product in 66% yield (entry 6). Finally, *n*-BuLi and *s*-BuLi were both tested under the optimized conditions (entries 8 and 9) with only *s*-BuLi providing the desired compound in a slightly reduced yield compared to *t*-BuLi (60 vs 66%). Applying these optimized conditions to our total synthesis worked effectively,

Table 1. Optimization of the Dehalogenation–Aromatization Model Reaction^a

entry	substrate	<i>t</i> -BuLi (equiv)	yield (%) ^b		
			20	21	22
1	20a (R = R' = <i>t</i> -Bu, X = Br)	2.0	29	7	2
2 ^c	20a (R = R' = <i>t</i> -Bu, X = Br)	2.0	21	21	8
3 ^{c,d}	20a (R = R' = <i>t</i> -Bu, X = Br)	3.0	23	33	13
4 ^{c,d}	20b (R = R' = <i>t</i> -Bu, X = Cl)	3.0	0	56	32
5 ^{c,d}	20c (R = H, R' = <i>t</i> -Bu, X = Cl)	4.0	20	38	N/A
6 ^c	20c (R = H, R' = <i>t</i> -Bu, X = Cl)	4.0	trace	66 ^e	N/A
7 ^c	20c (R = H, R' = <i>t</i> -Bu, X = Cl)	3.0	trace	49 ^e	N/A
8 ^c	20c (R = H, R' = <i>t</i> -Bu, X = Cl)	<i>n</i> -BuLi (4.0)	59 ^e	0	N/A
9 ^c	20c (R = H, R' = <i>t</i> -Bu, X = Cl)	<i>s</i> -BuLi (4.0)	trace	60 ^e	N/A

^aReaction conditions: **20** (0.05 mmol), THF (0.5 mL). ^bMeasured by ¹H NMR spectroscopy using 1,3,5-trimethoxybenzene as an internal standard. ^c*n*-hexane:THF (95:5) was used instead of THF. ^dInverse addition of lithium reagent was operated. ^eIsolated yields.

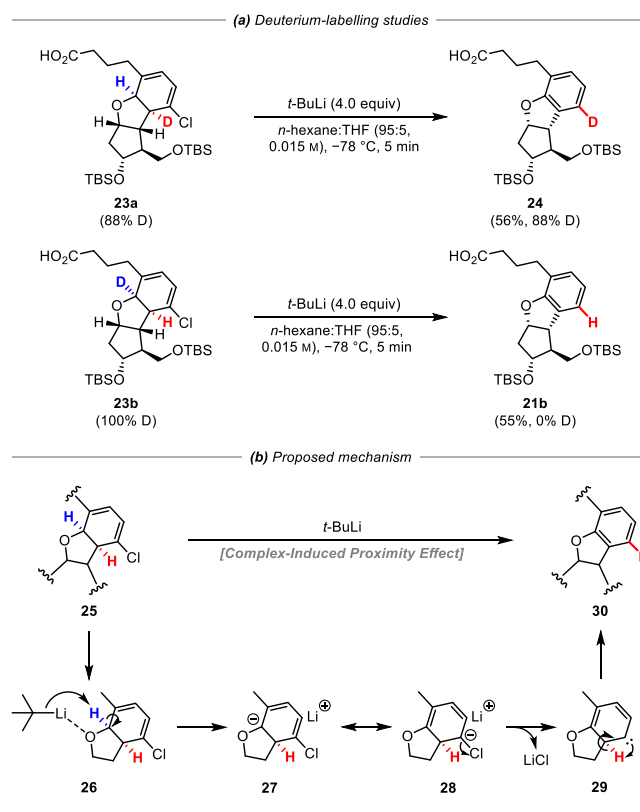
and the desired aromatic product **16** was obtained in 77% yield (Scheme 2c). Finally, treatment with TBAF effected deprotection of the TBS groups and afforded beraprost **1** in only 8 steps from enal-lactone **7** (14 steps LLS).

Mechanistic Studies of Aromatization. Having completed the total synthesis, we wanted to understand the mechanism of the intriguing dehalogenation–aromatization process and in particular the fate of the two hydrogen atoms at the pre-aromatized ring junction (Scheme 3a). Thus, mono-deuterated chlorocyclohexadienes **23a** and **23b** were prepared (see the Supporting Information for details), and each was treated with *t*-BuLi under the optimized reaction conditions. Chlorocyclohexadiene **23a** gave aromatized product **24** with complete incorporation of deuterium into the aromatic ring. In contrast, no deuterium was observed when isomer **23b** was used nor when the reaction was quenched with methanol-*d*₄. The 1,2-hydrogen atom shift that clearly occurred is likely to have resulted from the intermediacy of a carbene species.

Such a species could arise from an ether-directed deprotonation [complex-induced proximity effect (CIPE)] to give **27/28** followed by α -elimination to form carbene intermediate **29** (Scheme 3b).²⁶ The energy barrier for the resultant 1,2-hydrogen shift of this carbene was calculated to be almost barrierless (1 kcal mol⁻¹), which would make deprotonation the slowest step along this pathway. The fact that the chloride gave higher yields than the bromide suggests that lithium–halogen exchange, which would be more efficient with the bromide, is unlikely to be involved. Improved results using non-coordinating solvents also point to the importance of a complex-induced proximity effect to both break up any organolithium aggregates and direct deprotonation adjacent to the ether. The observation that *s*-BuLi was less effective and *n*-BuLi was ineffective to producing the desired aromatic product provides further evidence for our proposed mechanism since the reactivity of the various alkylolithiums to effect α -ether deprotonation decreases in the order of *t*-BuLi > *s*-BuLi \gg *n*-BuLi.²⁷

Modular Synthesis of Functionalized Indolines. We wanted to explore the generality of the novel IEDDA/

Scheme 3. Mechanistic Studies of Aromatization

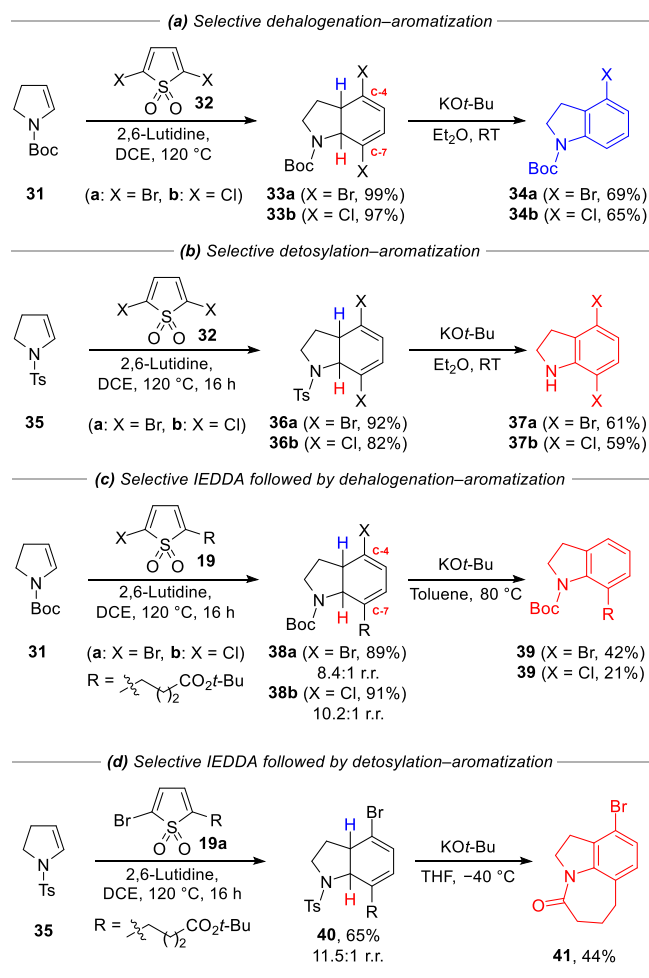


cheletropic extrusion and dehalogenation–aromatization process, in particular to determine whether it could be applied to the synthesis of the all-important indoline skeletons as well. In fact, this methodology could prove valuable in the synthesis of C-4/C-7 functionalized indoline scaffolds, which are commonly found in natural products and medicinal chemistry programs.²⁸ Most strategies for the synthesis of indolines focus either on the reduction of indoles or the synthesis of the 5-membered nitrogen heterocycle.²⁹ Very few of these

approaches target the aromatic ring, which would allow for a greater degree of modularity to be accessed in the synthesis of these important scaffolds.

The reaction of symmetrical 2,5-dihalogenated thiophene 1,1-dioxides **32a/b** with *N*-Boc-2,3-dihydropyrrole **31** gave dihalodienes **33a/b** in almost quantitative yield (Scheme 4).

Scheme 4. Synthesis of Mono- and Di-Halodienes and Their Selective Dehalogenation— or Detosylation—Aromatization Reactions

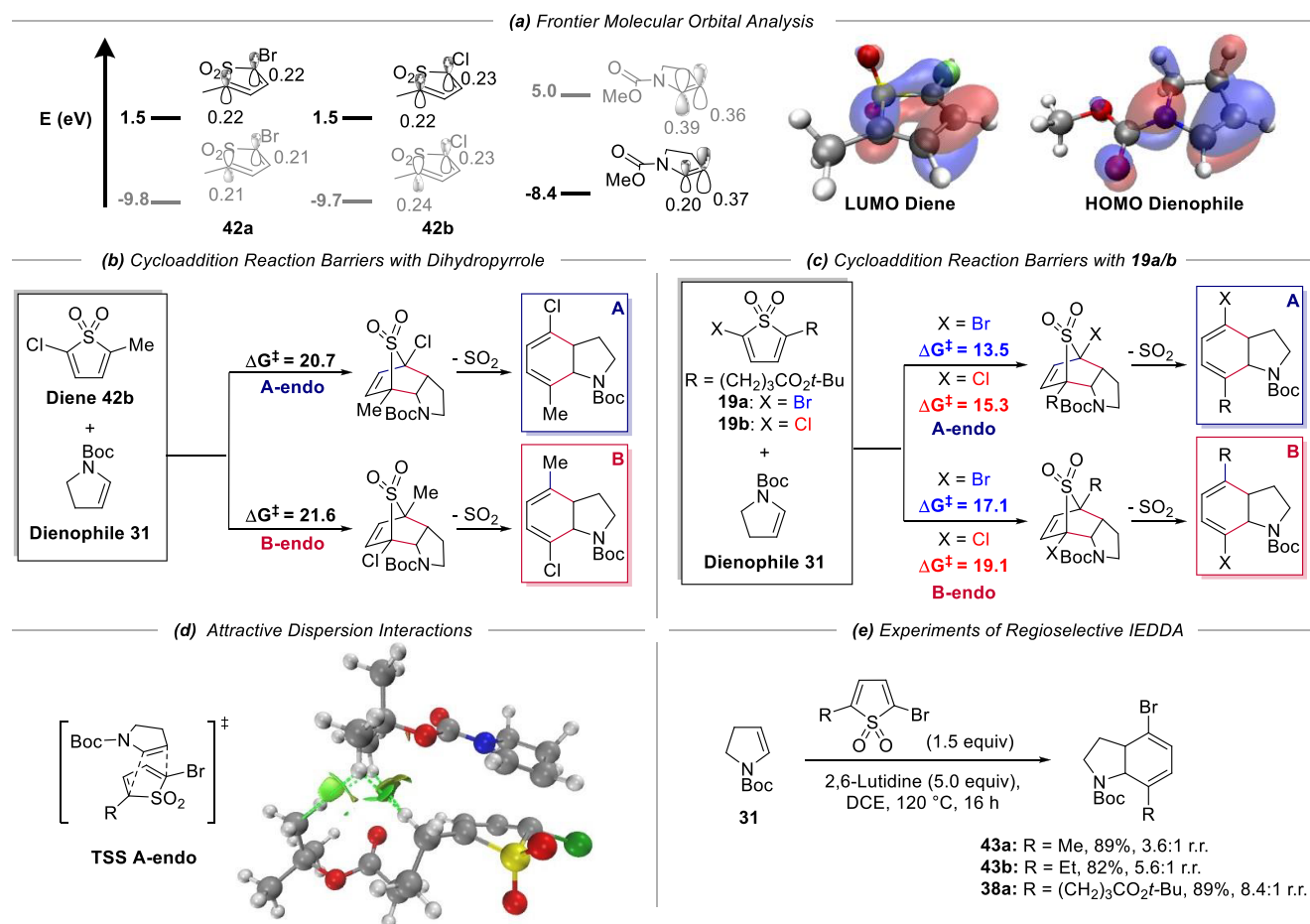


However, while subsequent treatment with *t*-BuLi led to a complex mixture, we found that reaction with potassium *tert*-butoxide (KO*t*-Bu) was able to effect dehalogenation—aromatization. In contrast to the dihydrofuran cycloadducts where deprotonation occurred adjacent to the oxygen, in this case, the proton distal to the nitrogen was removed giving 4-bromoindoline **34a** in good yield and as a single regioisomer (Scheme 4). The chlorodiene **33b** also worked equally well, giving **34b** as a single regioisomer. Using *N*-Ts-2,3-dihydropyrrole **35**, a different pathway for elimination—aromatization was available, enabling us to retain both halogens. Thus, following another high yielding IEDDA/cheletropic extrusion, cycloadducts **36a/b**, were obtained in 92% yield. Treatment with KO*t*-Bu now resulted in elimination of the tosyl group and led to dibromo- and dichloroindoline **37a** and **37b** in 61 and 59% yield, respectively. It is noteworthy that in the two substrate classes a different proton is removed: with **33a/b** the proton distal to the *N*-Boc group (blue proton)

is removed, whereas in the case of the **36a/b**, it is the proton proximal to the *N*-Ts group (red proton) that is removed.

Finally, we explored the IEDDA/cheletropic extrusion of unsymmetrical thiophene 1,1-dioxides **19a/b** with *N*-Boc-2,3-dihydropyrrole **31** and *N*-Ts-2,3-dihydropyrrole **35**. Surprisingly, in each case, this gave the adduct with high regioselectivity in which the alkyl chain was *syn* to the *N*-Boc/*N*-Ts group (the more hindered adduct). Subsequent treatment of cycloadducts **38a/b** with KO*t*-Bu unfortunately resulted in substantial quantities of elimination of the *N*-Boc group, likely due to the fact that the proton distal to the *N*-Boc group (blue proton) would be preferentially removed, by analogy with substrate **33a/b**. A brief optimization revealed that increased preference for the desired dehalogenation—aromatization process was observed in non-polar solvents and that the bromide behaved better than the chloride giving indoline **39** in 42% yield. A similar treatment of cycloadduct **40** with KO*t*-Bu also resulted in competing elimination, but nevertheless, elimination of the tosyl group followed by tautomerization and intramolecular amidation delivered aza-tricyclic **41** in 44% yield. It is notable that such aza-tricyclic skeletons are prevalent in many natural products and bioactive molecules.³⁰

Computational Studies of Regioselective IEDDA. The high regioselectivity observed in the IEDDA/cheletropic extrusion in favor of the more hindered adduct was unexpected and so we performed computational analysis to try to understand the origin of the selectivity. One possibility was that the cycloaddition was governed by electronic factors in which the polarity of the HOMO of the enamide matched the polarity of the LUMO of the diene. However, frontier molecular orbital calculations³¹ on a model dienophile, *N*-CO₂Me-2,3-dihydro-1*H*-pyrrole (truncated **31**), and model dienes, 2-methyl-5-halothiophene 1,1-dioxide, **42a/b** (truncated **19a/b**), showed that the LUMO lobes of the unsymmetrical diene, despite having very different electron donating and withdrawing groups attached, had similar coefficients at the two ends, indicating that there would be no preferred orientation, which can be seen when visualizing the relevant orbitals (Scheme 5a). Modeling the cycloaddition reaction between **31** and the same diene **42b** gave rise to two endo TSs (we established that the *endo* TSs were lower than the *exo* TSs in the reaction of diene **42b** with dihydrofuran – see ESI) in which the one where the Boc group was *syn* to the alkyl chain, leading to the observed and more hindered product, was 0.9 kcal mol⁻¹ lower in energy than the alternative where the Boc group was *anti* to the alkyl chain (Scheme 5b). This was not enough to account for the experimental selectivity seen, and so the *endo* TSs for the full system, **19a/b** as the diene and **31** as the dienophile, were modeled. They now showed a substantial difference in energy of ~3.5 kcal mol⁻¹ when London dispersion interactions were included. The London dispersion interactions were found to have contributed between 0.6 and 3.9 kcal mol⁻¹, depending on the level of theory with which they were studied. This suggests that a significant portion of the selectivity can be accounted for by London dispersion interactions, stabilizing the former TS (Scheme 5d), which is not present in the transition state with truncated diene 2-methyl-5-chlorothiophene 1,1-dioxide **42b**. This was verified experimentally: using smaller substituents on the diene (Me, Et) in place of the longer propyl ester led to progressively lower regioselectivity (Scheme 5e). It may seem unusual that LD interactions could

Scheme 5. Computational Studies of Regioselective IEDDA^a

^a(a) Frontier molecular orbital energies and coefficients (HF/6-31G). The lobes of reacting orbital coefficients are expected to match in magnitude to have a good overlap for reactivity. (b) Reaction energies for the cycloaddition reaction with dihydropyrrole. (c) Reaction energies for the cycloaddition reaction with 19a/19b. (d) Plot of noncovalent interactions (NCI)³² showing the weakly attractive van der Waals interaction consistent with LD forces in the TS of major isomer formation, which is absent in the TS of minor isomer formation (B3LYP/6-31G* with D3 dispersion correction and PCM solvation for dichloroethane). Dashed green lines have been included to indicate the location of the surfaces between the bulky alkyl groups. (e) Experiments of regioselective IEDDA.

lead to such high selectivity, but there are numerous cases where it is surprisingly large and can dominate selectivity.^{33,34} Our observations add to the growing recognition of the importance of London dispersion interactions contributing to selectivity in chemical reactions.³³

CONCLUSIONS

In conclusion, we have developed a highly stereoselective and modular synthesis of the potent anti-platelet agent, beraprost, in only 14 steps (LLS) in >99% e.e. The two sidechains of beraprost were readily introduced through a 1,4-conjugate addition of a higher-order cyanocuprate and a powerful IEDDA/chelotropic extrusion process, which produced a chloro-diene system that set the stage for a unique dehalogenation–aromatization reaction using *t*-BuLi. The chloride present in the thiophene 1,1-dioxide served a dual role: it inhibited cyclodimerization of the thiophene 1,1-dioxide and enabled a unique dehalogenation–aromatization. Mechanistic analysis of this step through deuterium-labeling studies showed the intermediacy of a carbene which underwent an aromatizing 1,2-hydrogen shift. Finally, we showed the applicability of our IEDDA/chelotropic extrusion and

dehalogenation–aromatization process to the synthesis of indolines. Reaction of symmetrical 2,5-dihalogenated thiophene 1,1-dioxides and 2,3-dihydropyrroles gave cycloadducts which underwent selective elimination–aromatization to afford either C-4 halogenated indolines or C-4/C-7 dihaloindolines depending on the nature of the nitrogen protecting group. Using nonsymmetrical 2-halo,5-alkyl thiophene 1,1-dioxides with 2,3-dihydropyrroles gave cycloadducts with high regioselectivity. Subsequent dehalogenation–aromatization then gave the C-7 indoline, providing a unique and modular approach to these medicinally relevant scaffolds.

ASSOCIATED CONTENT

Supporting Information

The Supporting Information is available free of charge at <https://pubs.acs.org/doi/10.1021/jacs.3c04582>.

Experimental procedures, spectroscopic data (1H NMR, 13C NMR, IR, HRMS) (PDF)

Geometry coordinates for calculated structures (XYZ)

Accession Codes

CCDC 2172054 and 2226750 contain the supplementary crystallographic data for this paper. These data can be obtained free of charge via www.ccdc.cam.ac.uk/data_request/cif, or by emailing data_request@ccdc.cam.ac.uk, or by contacting The Cambridge Crystallographic Data Centre, 12 Union Road, Cambridge CB2 1EZ, UK; fax: +44 1223 336033.

CCDC 2172054 (7) and 2226750 (41) contain the supplementary crystallographic data for this paper. These data can be obtained free of charge via www.ccdc.cam.ac.uk/data_request/cif, or by emailing data_request@ccdc.cam.ac.uk, or by contacting The Cambridge Crystallographic Data Centre, 12 Union Road, Cambridge CB2 1EZ, UK; fax: +44 1223 336033.

AUTHOR INFORMATION

Corresponding Author

Varinder K. Aggarwal – School of Chemistry, University of Bristol, Cantock's Close, Bristol BS8 1TS, U.K.;
orcid.org/0000-0003-0344-6430; Email: v.aggarwal@bristol.ac.uk

Authors

Ze-Shu Wang – School of Chemistry, University of Bristol, Cantock's Close, Bristol BS8 1TS, U.K.
Steven H. Bennett – School of Chemistry, University of Bristol, Cantock's Close, Bristol BS8 1TS, U.K.
Bilal Kicin – School of Chemistry, University of Bristol, Cantock's Close, Bristol BS8 1TS, U.K.
Changcheng Jing – School of Chemistry, University of Bristol, Cantock's Close, Bristol BS8 1TS, U.K.
Johan A. Pradeilles – School of Chemistry, University of Bristol, Cantock's Close, Bristol BS8 1TS, U.K.;
orcid.org/0000-0003-0895-3239
Karen Thai – School of Chemistry, University of Bristol, Cantock's Close, Bristol BS8 1TS, U.K.
James R. Smith – School of Chemistry, University of Bristol, Cantock's Close, Bristol BS8 1TS, U.K.
P. David Bacoş – School of Chemistry, University of Bristol, Cantock's Close, Bristol BS8 1TS, U.K.;
orcid.org/0000-0002-7288-2730
Valerio Fasano – School of Chemistry, University of Bristol, Cantock's Close, Bristol BS8 1TS, U.K.
Carla M. Saunders – School of Chemistry, University of Bristol, Cantock's Close, Bristol BS8 1TS, U.K.

Complete contact information is available at:
<https://pubs.acs.org/10.1021/jacs.3c04582>

Author Contributions

[§]Z.-S.W., S.H.B., and B.K. contributed equally to this work.

Notes

The authors declare no competing financial interest.

ACKNOWLEDGMENTS

We thank EPSRC (EP/M012530/1) for financial support. V.F. thanks the University of Bristol for awarding the EPSRC Doctoral Prize Fellowship (EP/R513179/1). Z.-S.W. thanks the Foundation of Wenzhou Science and Technology Bureau (No. ZY2020027) for financial support. We thank Dr. Hazel A. Sparkes and Dr. Natalie E. Pridmore for X-ray analysis and Dr. Natalie Fey for helpful discussions of the computational results. This work was carried out using the computational

facilities of the Advanced Computing Research Centre, University of Bristol - <http://www.bristol.ac.uk/acrc/>.

REFERENCES

- (1) (a) Galiè, N.; Torbicki, A.; Barst, R.; Darteville, P.; Haworth, S.; Higenbottam, T.; Olschewski, H.; Peacock, A.; Pietra, G.; Rubin, L. J.; Simonneau, G. Guidelines on diagnosis and treatment of pulmonary arterial hypertension: The Task Force on Diagnosis and Treatment of Pulmonary Arterial Hypertension of the European Society of Cardiology. *Eur. Heart J.* **2004**, *25*, 2243–2278. (b) Ruan, C.-H.; Dixon, R. A. F.; Willerson, J. T.; Ruan, K.-H. Prostacyclin Therapy for Pulmonary Arterial Hypertension. *Tex. Heart Inst. J.* **2010**, *37*, 391–399.
- (2) Sitbon, O.; Noordegraaf, A. V. Epoprostenol and Pulmonary Arterial Hypertension: 20 Years of Clinical Experience. *Eur. Respir. Rev.* **2017**, *26*, 160055–160069.
- (3) (a) Lucas, F. V.; Skrinska, V. A.; Chisolm, G. M.; Hesse, B. L. Stability of Prostacyclin in Human and Rabbit Whole Blood and Plasma. *Thromb. Res.* **1986**, *43*, 379–387. (b) Wong, P. Y.; Lee, W. H.; Chao, P. H.; Reiss, R. F.; McGiff, J. C. Metabolism of Prostacyclin by 9-Hydroxyprostaglandin Dehydrogenase in Human Platelets. Formation of a Potent Inhibitor of Platelet Aggregation and Enzyme Purification. *J. Biol. Chem.* **1980**, *255*, 9021–9024.
- (4) Belch, J. J. F.; McLaren, M.; Lau, C. S.; Mackay, I. R.; Bancroft, A.; McEwen, J.; Thompson, J. M. Cicaprost, an Orally Active Prostacyclin Analogue: Its Effects on Platelet Aggregation and Skin Blood Flow in Normal Volunteers. *Br. J. Clin. Pharmacol.* **1993**, *35*, 643–647.
- (5) (a) Schrör, K.; Darius, H.; Matzky, R.; Ohlendorf, R. The Antiplatelet and Cardiovascular Actions of a New Carbacyclin Derivative (ZK 36 374) — Equipotent to PGI₂ in Vitro. *Naunyn-Schmiedeberg's Arch. Pharmacol.* **1981**, *316*, 252–255. (b) Casals-Stenzel, J.; Buse, M.; Losert, W. Comparison of the Vasodepressor Action of ZK 36 374, a Stable Prostacyclin Derivative, PGI₂ and PGE₁ with Their Effect on Platelet Aggregation and Bleeding Time in Rats. *Prostaglandins, Leukotrienes Med.* **1983**, *10*, 197–212.
- (6) (a) Bannai, K.; Toru, T.; Ōba, T.; Tanaka, T.; Okamura, N.; Watanabe, K.; Hazato, A.; Kurozumi, S. Synthesis of Chemically Stable Prostacyclin Analogs. *Tetrahedron* **1983**, *39*, 3807–3819. (b) Bannai, K.; Toru, T.; Ōba, T.; Tanaka, T.; Okamura, N.; Watanabe, K.; Hazato, A.; Kurozumi, S. Synthesis of Chemically Stable PGI₂ Analogs II - Synthesis of Halogen Substituted PGI₂ Analogs. *Tetrahedron* **1986**, *42*, 6735–6746. (c) Skuballa, W.; Schillinger, E.; Stürzbecher, C. S.; Vorbrüggen, H. Prostaglandin Analogs. Part 9. Synthesis of a New Chemically and Metabolically Stable Prostacyclin Analog with High and Long-Lasting Oral Activity. *J. Med. Chem.* **1986**, *29*, 313–315. (d) Nakano, T.; Makino, M.; Morizawa, Y.; Matsumura, Y. Synthesis of Novel Difluoroprostacyclin Derivatives: Unprecedented Stabilizing Effect of Fluorine Substituents. *Angew. Chem., Int. Ed.* **1996**, *35*, 1019–1021.
- (7) Melian, E. B.; Goa, K. L. Beraprost. *Drugs* **2002**, *62*, 107–133.
- (8) (a) Wakita, H.; Yoshiwara, H.; Tajima, A.; Kitano, Y.; Nagase, H. Preparative Resolution of a Key Intermediate for the Synthesis of Optically Active *m*-Phenylene PGI₂ Derivatives. *Tetrahedron: Asymmetry* **1999**, *10*, 4099–4105. (b) Wakita, H.; Yoshiwara, H.; Nishiyama, H.; Nagase, H. Total Synthesis of Optically Active *m*-Phenylene PGI₂ Derivative: Beraprost. *Heterocycles* **2000**, *53*, 1085–1110. (c) Wakita, H.; Yoshiwara, H.; Kitano, Y.; Nishiyama, H.; Nagase, H. Preparative Resolution of 2-Methyl-4-Hexynic Acid for the Synthesis of Optically Active *m*-Phenylene PGI₂ Derivatives and Determination of Their Absolute Configuration. *Tetrahedron: Asymmetry* **2000**, *11*, 2981–2989. (d) Reddy, K. N.; Vijaykumar, B. V. D.; Chandrasekhar, S. Formal Synthesis of Antiplatelet Drug, Beraprost. *Org. Lett.* **2012**, *14*, 299–301.
- (9) (a) Liu, X.; Tian, C.; Jiao, X.; Li, X.; Yang, H.; Yao, Y.; Xie, P. A Practical Synthesis of Chiral Tricyclic Cyclopenta[*b*]benzofuran, a Key Intermediate of Beraprost. *Org. Biomol. Chem.* **2016**, *14*, 7715. (b) Sharma, V.; Batra, H.; Tuladhar, S. Method of Producing Beraprost. *Inter. Pat. Appl. WO2017027706*, 20 Dec, 2012.

- (10) Umemiya, S.; Sakamoto, D.; Kawauchi, G.; Hayashi, Y. Enantioselective Total Synthesis of Beraprost Using Organocatalyst. *Org. Lett.* **2017**, *19*, 1112–1115.
- (11) For a recent, transition-metal catalyzed, asymmetric route to construct the cyclopentane core and its applications to prostaglandins, see: Zhang, F.; Zeng, J.; Gao, M.; Wang, L.; Chen, G.-Q.; Lu, Y.; Zhang, X. Concise, Scalable and Enantioselective Total Synthesis of Prostaglandins. *Nat. Chem.* **2021**, *13*, 692–697.
- (12) (a) Coulthard, G.; Erb, W.; Aggarwal, V. K. Stereocontrolled Organocatalytic Synthesis of Prostaglandin PGF_{2α} in Seven Steps. *Nature* **2012**, *489*, 278–281. (b) Prévost, S.; Thai, K.; Schützenmeister, N.; Coulthard, G.; Erb, W.; Aggarwal, V. K. Synthesis of Prostaglandin Analogues, Latanoprost and Bimatoprost, Using Organocatalysis via a Key Bicyclic Enal Intermediate. *Org. Lett.* **2015**, *17*, 504–507. (c) Baars, H.; Classen, M. J.; Aggarwal, V. K. Synthesis of Alfaprostol and PGF_{2α} through 1,4-Addition of an Alkyne to an Enal Intermediate as the Key Step. *Org. Lett.* **2017**, *19*, 6008–6011. (d) Pelšs, A.; Gandhamsetty, N.; Smith, J. R.; Mailhol, D.; Silvi, M.; Watson, A.; Perez-Powell, I.; Prévost, S.; Schützenmeister, N.; Moore, P. R.; Aggarwal, V. K. Reoptimization of the Organocatalyzed Double Aldol Domino Process to a Key Enal Intermediate and its Application to the Total Synthesis of Δ¹²-Prostaglandin J₃. *Chem. - Eur. J.* **2018**, *24*, 9542–9545. (e) Jing, C.; Mallah, S.; Kriemen, E.; Bennett, S. H.; Fasano, V.; Lennox, A. J. J.; Hers, I.; Aggarwal, V. K. Synthesis, Stability, and Biological Studies of Fluorinated Analogues of Thromboxane A₂. *ACS Cent. Sci.* **2020**, *6*, 995–1000. (f) Bennett, S. H.; Coulthard, G.; Aggarwal, V. K. Prostaglandin Total Synthesis Enabled by the Organocatalytic Dimerization of Succinaldehyde. *Chem. Rec.* **2020**, *20*, 936–947. (g) Jing, C.; Aggarwal, V. K. Total Synthesis of Thromboxane B₂ via a Key Bicyclic Enal Intermediate. *Org. Lett.* **2020**, *22*, 6505–6509. (h) Bennett, S. H.; Aggarwal, V. K. Organocatalytic Dimerization of Succinaldehyde. *Org. Synth.* **2022**, *99*, 139.
- (13) (a) Bailey, W. J.; Cummins, E. W. Cyclic Dienes. IV. The Dimerization of Thiophene 1-Dioxide. *J. Am. Chem. Soc.* **1954**, *7*, 1936–1939. (b) Bailey, W. J.; Cummins, E. W. Cyclic Dienes. V. Diels-Alder Reactions of Thiophene 1-Dioxide. *J. Am. Chem. Soc.* **1954**, *7*, 1940–1942. (c) Nakayama, J.; Sugihara, Y. *Chemistry of Thiophene 1,1-Dioxides in Organosulfur Chemistry II in Topics in Current Chemistry*; Page, P. C. B., Ed.; Springer: Berlin, Heidelberg, 1999; Vol. 205, pp 131–195. (d) Lu, Y.; Dong, Z.; Wang, P.; Zhou, H.-B. *Thiophene Oxidation and Reduction Chemistry in Thiophenes in Topics in Heterocyclic Chemistry*; Joule, J. A., Ed.; Springer: Berlin, Heidelberg, 2015; Vol. 39, pp 227–293. (e) Miyahara, Y.; Inazu, T. An Extremely Efficient Synthesis of Thiophene 1,1-Dioxides. Oxidation of Thiophene Derivatives with Dimethyldioxirane. *Tetrahedron Lett.* **1990**, *31*, 5955–5958. (f) Nakayama, J.; Nagasawa, H.; Sugihara, Y.; Ishii, A. Synthesis, Isolation, and Full Characterization of the Parent Thiophene 1,1-Dioxide. *J. Am. Chem. Soc.* **1997**, *119*, 9077–9078.
- (14) For impressive recent publications on the use of non-symmetrical thiophene 1,1-dioxides in total synthesis, see: (a) Park, K. H. K.; Frank, N.; Duarte, F.; Anderson, E. A. Collective Synthesis of Illudalane Sesquiterpenes via Cascade Inverse Electron Demand (4 + 2) Cycloadditions of Thiophene S,S-Dioxides. *J. Am. Chem. Soc.* **2022**, *144*, 10017–10024. (b) Kabuki, A.; Yamaguchi, J. Formal Syntheses of Dictyodendrins B, C, and E by a Multi-Substituted Indole Synthesis. *Synthesis* **2022**, *54*, 4963–4970.
- (15) Mukherjee, S.; Lee, D. Application of Tandem Ring-Closing Enyne Metathesis: Formal Total Synthesis of (–)-Cochleamycin A. *Org. Lett.* **2009**, *11*, 2916–2919.
- (16) Hayashi, Y.; Kojima, M.; Yasui, Y.; Kanda, Y.; Mukaiyama, T.; Shomura, H.; Nakamura, D.; Ritmaleni; Sato, I. Diarylprolinol in an Asymmetric, Direct Cross-Aldol Reaction with Alkynyl Aldehydes. *ChemCatChem* **2013**, *5*, 2887–2892.
- (17) Illa, O.; Arshad, M.; Ros, A.; McGarrigle, E. M.; Aggarwal, V. K. Practical and Highly Selective Sulfur Ylide-Mediated Asymmetric Epoxidations and Aziridinations Using a Cheap and Readily Available Chiral Sulfide. Application to the Total Synthesis of Quinine and Quinidine. *J. Am. Chem. Soc.* **2010**, *132*, 1828–1830.
- (18) (a) Iosub, A. V.; Stahl, S. S. Palladium-Catalyzed Aerobic Oxidative Dehydrogenation of Cyclohexenes to Substituted Arene Derivatives. *J. Am. Chem. Soc.* **2015**, *137*, 3454–3457. (b) Horrillo-Martínez, P.; Virolleaud, M.-A.; Jaekel, C. Selective Palladium-Catalyzed Dehydrogenation of Limonene to Dimethylstyrene. *ChemCatChem* **2010**, *2*, 175–181.
- (19) (a) Ikeda, S.-i.; Mori, N.; Sato, Y. Regioselective Cyclic Cotrimerization of α,β-Enones and Alkynes by a Nickel–Aluminum Catalyst System. *J. Am. Chem. Soc.* **1997**, *119*, 4779–4780. (b) Lu, Z.; Li, Y.; Deng, J.; Li, A. Total Synthesis of the Daphniphyllum Alkaloid Daphenylline. *Nat. Chem.* **2013**, *5*, 679–684.
- (20) (a) London, G.; von Wantoch Rekowski, M.; Dumele, O.; Schweizer, W. B.; Gisselbrecht, J.-P.; Boudon, C.; Diederich, F. Pentalenes with Novel Topologies: Exploiting the Cascade Carbopalladation Reaction between Alkynes and Gem-Dibromoolefins. *Chem. Sci.* **2014**, *5*, 965–972. (b) Geist, E.; Berneaud-Kötz, H.; Baikstis, T.; Dräger, G.; Kirschning, A. Toward Chromanes by de Novo Construction of the Benzene Ring. *Org. Lett.* **2019**, *21*, 8930–8933.
- (21) Revés, M.; Ferrer, C.; León, T.; Doran, S.; Etayo, P.; Vidal-Ferran, A.; Riera, A.; Verdager, X. Primary and Secondary Aminophosphines as Novel P-Stereogenic Building Blocks for Ligand Synthesis. *Angew. Chem., Int. Ed.* **2010**, *49*, 9452–9455.
- (22) Mashraqui, S.; Keehn, P. Active MnO₂. Oxidative Dehydrogenations. *Synth. Commun.* **1982**, *12*, 637–645.
- (23) Chen, W.; Chen, Y.; Gu, X.; Chen, Z.; Ho, C.-Y. (NHC)Pd(II) Hydride-Catalyzed Dehydroaromatization by Olefin Chain-Walking Isomerization and Transfer-Dehydrogenation. *Nat. Commun.* **2022**, *13*, 5507.
- (24) (a) Raasch, M. S. Addition–Rearrangement Reactions of Halogenated Thiophene Dioxides with Furans. *J. Org. Chem.* **1980**, *45*, 867–870. (b) Nakayama, J.; Yamaoka, S.; Nakanishi, T.; Hoshino, M. 3,4-Di-*tert*-butylthiophene 1,1-dioxide, a Convenient Precursor of *o*-Di-*tert*-butylbenzene and its Derivatives. *J. Am. Chem. Soc.* **1988**, *110*, 6598–6599. (c) Moiseev, A. M.; Balenkova, E. S.; Nenajdenko, V. G. Reactions of Electron-Withdrawing Thiophene 1,1-dioxides with Furans. A Novel Reaction Pathway. *Russ. Chem. Bull.* **2006**, *55*, 712–717.
- (25) (a) Clayden, J.; Menet, C. J. 2,3-Dihydroisindolones by Cyclisation and Rearomatisation of Lithiated Benzamides. *Tetrahedron Lett.* **2003**, *44*, 3059–3062. (b) Knölker, H.-J.; Filali, S. Transition Metal Complexes in Organic Synthesis, Part 69. [1] Total Synthesis of the Amaryllidaceae Alkaloids Anhydrolycorinine and Hippadine Using Iron- and Palladium-Mediated Coupling Reactions. *Synlett* **2003**, *11*, 1752–1754. (c) Kondratov, I. S.; Tolmacheva, N. A.; Dolovanyuk, V. G.; Gerus, I. I.; Daniliuc, C.-G.; Haufe, G. Synthesis of Trifluoromethyl-Containing Polysubstituted Aromatic Compounds by Diels–Alder Reaction of Ethyl 3-Benzamido-2-oxo-6-(trifluoromethyl)-2H-pyran-5-carboxylate. *Eur. J. Org. Chem.* **2015**, *2015*, 2482–2491.
- (26) Whisler, M. C.; MacNeil, S.; Snieckus, V.; Beak, P. Beyond Thermodynamic Acidity: A Perspective on the Complex-Induced Proximity Effect (CIPE) in Deprotonation Reactions. *Angew. Chem., Int. Ed.* **2004**, *43*, 2206–2225.
- (27) Fitt, J. J.; Gschwend, H. W. Reaction of *n*-, *sec*-, and *tert*-Butyllithium with Dimethoxyethane (DME): A Correction. *J. Org. Chem.* **1984**, *49*, 209–210.
- (28) (a) Axten, J. M.; Romeril, S. P.; Shu, A.; Ralph, J.; Medina, J. R.; Feng, Y.; Li, W. H. H.; Grant, S. W.; Heerding, D. A.; Minthorn, E.; Mencken, T.; Gaul, N.; Goetz, A.; Stanley, T.; Hassell, A. M.; Gampe, R. T.; Atkins, C.; Kumar, R. Discovery of GSK2656157: An Optimized PERK Inhibitor Selected for Preclinical Development. *ACS Med. Chem. Lett.* **2013**, *4*, 964–968. (b) Zeeli, S.; Weill, T.; Finkin-Groner, E.; Bejar, C.; Melamed, M.; Furman, S.; Zhenin, M.; Nudelman, A.; Weinstock, M. Synthesis and Biological Evaluation of Derivatives of Indoline as Highly Potent Antioxidant and Anti-inflammatory Agents. *J. Med. Chem.* **2018**, *61*, 4004–4019. (c) Yang,

Y.; Wang, K.; Chen, H.; Feng, Z. Design, Synthesis, Evaluation, and SAR of 4-Phenylindoline Derivatives, a Novel Class of Small-Molecule Inhibitors of the Programmed Cell Death-1/ Programmed Cell Death-Ligand 1 (PD-1/PD-L1) Interaction. *Eur. J. Med. Chem.* **2021**, *211*, 113001–113021.

(29) (a) Liu, D.; Zhao, G.; Xiang, L. Diverse Strategies for the Synthesis of the Indoline Scaffold. *Eur. J. Org. Chem.* **2010**, *2010*, 3975–3984. (b) Silva, T. S.; Rodrigues, M. T., Jr.; Santos, H.; Zeoly, L. A.; Almeida, W. P.; Barcelos, R. C.; Gomes, R. C.; Fernandes, F. S.; Coelho, F. Recent Advances in Indoline Synthesis. *Tetrahedron* **2019**, *75*, 2063–2097.

(30) For selected examples on natural products and bioactive molecules containing aza-tricyclic skeletons, see: (a) Mandal, P. K.; Gao, F.; Lu, Z.; Ren, Z.; Ramesh, R.; Birtwistle, J. S.; Kaluarachchi, K. K.; Chen, X.; Bast, R. C.; Liao, W. S.; McMurray, J. S. Potent and Selective Phosphopeptide Mimetic Prodrugs Targeted to the Src Homology 2 (SH2) Domain of Signal Transducer and Activator of Transcription 3. *J. Med. Chem.* **2011**, *54*, 3549–3563. (b) Willoughby, C. A.; Bull, H. G.; Garcia-Calvo, M.; Jiang, J.; Chapman, K. T.; Thornberry, N. A. Discovery of Potent, Selective Human Granzyme B Inhibitors That Inhibit CTL Mediated Apoptosis. *Bioorg. Med. Chem. Lett.* **2002**, *12*, 2197–2200.

(31) Ess, D.; Jones, G.; Houk, K. Conceptual, Qualitative, and Quantitative Theories of 1,3-Dipolar and Diels–Alder Cycloadditions Used in Synthesis. *Adv. Synth. Catal.* **2006**, *348*, 2337–2361.

(32) Johnson, E. R.; Keinan, S.; Mori-Sánchez, P.; Contreras-García, J.; Cohen, A. J.; Yang, W. Revealing Noncovalent Interactions. *J. Am. Chem. Soc.* **2010**, *132*, 6498–6506.

(33) (a) Wagner, J. P.; Schreiner, P. R. London Dispersion in Molecular Chemistry—Reconsidering Steric Effects. *Angew. Chem., Int. Ed.* **2015**, *54*, 12274–12296. (b) McFord, A. W.; Butts, C. P.; Fey, N.; Alder, R. W. 3× Axial vs 3× Equatorial: The ΔG_{GA} Value Is a Robust Computational Measure of Substituent Steric Effects. *J. Am. Chem. Soc.* **2021**, *143*, 13573–13578.

(34) For example, in the cycloaddition shown below, the apparently sterically more hindered product was obtained, favored by London dispersion attraction between the two large alkyl groups in the transition structure (a) Aikawa, H.; Takahira, Y.; Yamaguchi, M. Synthesis of 1,8-Di(1-adamantyl)naphthalenes as Single Enantiomers Stable at Ambient Temperatures. *Chem. Commun.* **2011**, *47*, 1479–1481. An alternative explanation for this aryne selectivity could also be a “stepwise,” nucleophilic addition connecting the two less hindered carbons followed by ring closure (b) Garr, A. N.; Luo, D.; Brown, N.; Cramer, C. J.; Buszek, K. R.; VanderVelde, D. Experimental and Theoretical Investigations into the Unusual Regioselectivity of 4,5-, 5,6-, and 6,7-Indole Aryne Cycloadditions. *Org. Lett.* **2010**, *12*, 96–99.